Subunit Q Is Required to Stabilize the Large Complex of NADPH Dehydrogenase in *Synechocystis* sp. Strain PCC 6803[1]

Jiaohong Zhao[2], Weiqiong Rong[2], Fudan Gao[2], Teruo Ogawa, and Weimin Ma*

College of Life and Environment Sciences, Shanghai Normal University, Shanghai 200234, China (J.Z., W.R., F.G., W.M.); and Bioscience Center, Nagoya University, Chikusa, Nagoya 464–8601, Japan (T.O.)

ORCID IDs: 0000-0002-8882-5968 (F.G.); 0000-0001-6061-8273 (T.O.); 0000-0003-4964-415X (W.M.).

Two major complexes of NADPH dehydrogenase (NDH-1) have been identified in cyanobacteria. A large complex (NDH-1L) contains NdhD1, NdhF1, and NdhP, which are absent in a medium size complex (NDH-1M). They play important roles in respiration, NDH-1-dependent cyclic electron transport around photosystem I, and CO_2 uptake. Two mutants sensitive to high light for growth and impaired in cyclic electron transport around photosystem I were isolated from the cyanobacterium *Synechocystis* sp. strain PCC 6803 transformed with a transposon-bearing library. Both mutants had a tag in an open reading frame encoding a product highly homologous to NdhQ, a single-transmembrane small subunit of the NDH-1L complex, identified in *Thermosynechococcus elongatus* by proteomics strategy. Deletion of *ndhQ* disassembled about one-half of the NDH-1L to NDH-1M and consequently impaired respiration, but not CO_2 uptake. During prolonged incubation of the thylakoid membrane with *n*-dodecyl-β-D-maltoside at room temperature, the rest of the NDH-1L in Δ*ndhQ* was disassembled completely to NDH-1M and was much faster than in the wild type. In the *ndhP*-deletion mutant (Δ*ndhP*) background, absence of NdhQ almost completely disassembled the NDH-1L to NDH-1M, similar to the results observed in the Δ*ndhD1*/Δ*ndhD2* mutant. We therefore conclude that both NdhQ and NdhP are essential to stabilize the NDH-1L complex.

Cyanobacterial NADPH dehydrogenase (NDH-1) complexes are localized in the thylakoid membrane (Ohkawa et al., 2001, 2002; Zhang et al., 2004; Xu et al., 2008; Battchikova et al., 2011a) and participate in a variety of bioenergetic reactions, such as respiration, cyclic electron transport around PSI, and CO_2 uptake (Ogawa, 1991; Mi et al., 1992; Ohkawa et al., 2000). Structurally, the cyanobacterial NDH-1 complexes closely resemble energy-converting complex I in eubacteria and the mitochondrial respiratory chain, regardless of the absence of homologs of three subunits in cyanobacterial genomes that constitute the catalytically active core of complex I (Friedrich et al., 1995; Friedrich and Scheide, 2000; Arteni et al., 2006). Over the past few years, significant achievements have been made in resolving the subunit compositions and functions of the multiple NDH-1 complexes in several cyanobacterial strains (for review, see Battchikova and Aro, 2007; Ogawa and Mi, 2007; Ma, 2009; Battchikova et al., 2011b; Ma and Ogawa, 2015). Four types of NDH-1 have been identified in the cyanobacterium *Synechocystis* sp. strain PCC 6803 (hereafter, *Synechocystis* 6803), and all four types of NDH-1 are involved in NDH-1-dependent cyclic electron transport (CET) around PSI (NDH-CET; Bernát et al., 2011). The NDH-CET plays an important role in coping with various environmental stresses, regardless of its elusive mechanism. For example, this function can greatly alleviate high light-sensitive growth phenotypes (Endo et al., 1999; Battchikova et al., 2011a; Dai et al., 2013; Zhang et al., 2014; Zhao et al., 2014). Therefore, high light strategy can help in identifying the proteins essential to NDH-CET.

Proteomics studies revealed the presence of three major NDH-1 complexes in cyanobacteria: a large complex (NDH-1L), a medium size complex (NDH-1M), and a small complex (NDH-1S) with molecular masses of about 460, 350, and 200 kD, respectively (Herranen et al., 2004). NDH-1M consists of 14 subunits (i.e. NdhA–NdhC, NdhE, NdhG–NdhO, and NdhS). In addition to these subunits, the NDH-1L complex contains NdhD1, NdhF1, NdhP, and NdhQ (Prommeenate et al., 2004; Battchikova et al., 2005, 2011b; Zhang et al., 2005, 2014; Nowaczyk et al., 2011; Wulfhorst et al., 2014; Ma and Ogawa, 2015) and is involved in respiration (Zhang et al., 2004). NDH-1S is composed of NdhD3, NdhF3, CO_2 uptake A (CupA), and CupS (Ogawa and Mi, 2007) and is considered to

[1] This work was supported by the National Natural Science Foundation of China (grant no. 31370270) and the Shanghai Natural Science Foundation (grant no. 14ZR1430000).

[2] These authors contributed equally to the article.

* Address correspondence to wma@shnu.edu.cn.

The author responsible for distribution of materials integral to the findings presented in this article in accordance with the policy described in the Instructions for Authors (www.plantphysiol.org) is: Weimin Ma (wma@shnu.edu.cn).

W.M. designed and supervised the experiments; J.Z. and W.R. performed the molecular and physiological experiments; F.G. performed the biochemical experiments; J.Z., W.R., and F.G. analyzed the data; T.O. and W.M. analyzed and interpreted the data; T.O. and W.M. wrote the article.

www.plantphysiol.org/cgi/doi/10.1104/pp.15.00503

be associated with NDH-1M in the cells as a functional complex NDH-1MS (Zhang et al., 2004, 2005) participating in CO_2 uptake. Among the several copies of *ndhD* and *ndhF* genes found in cyanobacterial genomes, *ndhD1* and *ndhF1* show the highest homology to chloroplast *ndhD* and *ndhF* genes, respectively, and CupA and CupS subunits of the cyanobacteria have no counterparts in higher plants. These facts suggest that the structure and composition of NDH-1L, but not the NDH-1MS complex, are similar to those of the chloroplast NDH-1 complex (Battchikova and Aro, 2007; Ogawa and Mi, 2007; Shikanai, 2007; Ma, 2009; Suorsa et al., 2009; Battchikova et al., 2011b; Ifuku et al., 2011; Peng et al., 2011a; Ma and Ogawa, 2015). Despite their similarity, a large number of subunits that constitute the chloroplast NDH-1 complex, including ferredoxin-binding subcomplex subunits NdhT and NdhU and all the subunits of subcomplex B and lumen subcomplex, are absent in the cyanobacterial NDH-1L complex (Battchikova et al., 2011b; Ifuku et al., 2011; Peng et al., 2011a). This implies that the stabilization strategies for the cyanobacterial NDH-1L complex and chloroplastic NDH-1 complex might be significantly different.

Recently, a new oxygenic photosynthesis-specific small subunit NdhQ was identified in the NDH-1L complex purified by Ni^{2+} affinity chromatography from *Thermosynechococcus elongatus* (Nowaczyk et al., 2011). NdhQ is extensively present in cyanobacteria, but its homolog is absent in higher plants (Nowaczyk et al., 2011). In this study, we demonstrate that deletion of NdhQ disassembled the NDH-1L into NDH-1M, but not NDH-1MS, in *Synechocystis* 6803 and consequently impaired respiration, but not CO_2 uptake. NdhQ and NdhP stabilize the NDH-1L complex. Thus, the stabilization strategy of cyanobacterial NDH-1L is distinctly different from that of the chloroplastic NDH-1 complex.

RESULTS

Isolation of NDH-CET-Defective Mutants

The NDH-CET has a protective role against high light stress in cyanobacteria (Battchikova et al., 2011a; Dai et al., 2013; Zhang et al., 2014; Zhao et al., 2014) and higher plants (Endo et al., 1999). Under high light conditions, therefore, the growth of NDH-CET-defective mutants is markedly retarded compared with the wild type, despite similar growth under moderate light irradiation. To screen for NDH-CET-defective mutants, we transformed wild-type cells with a transposon-bearing library, thus tagging and inactivating many genes randomly, and then cultured the mutant cells under high light conditions. We isolated two mutants, which were unable to grow on the plate under high light but grew similarly to the wild type under growth light (Fig. 1A).

To investigate whether the high light-sensitive growth phenotype of the two mutants resulted from defective NDH-CET, we monitored the postillumination rise in Chl *a* fluorescence. This approach has been extensively used to monitor NDH-CET activity in cyanobacteria

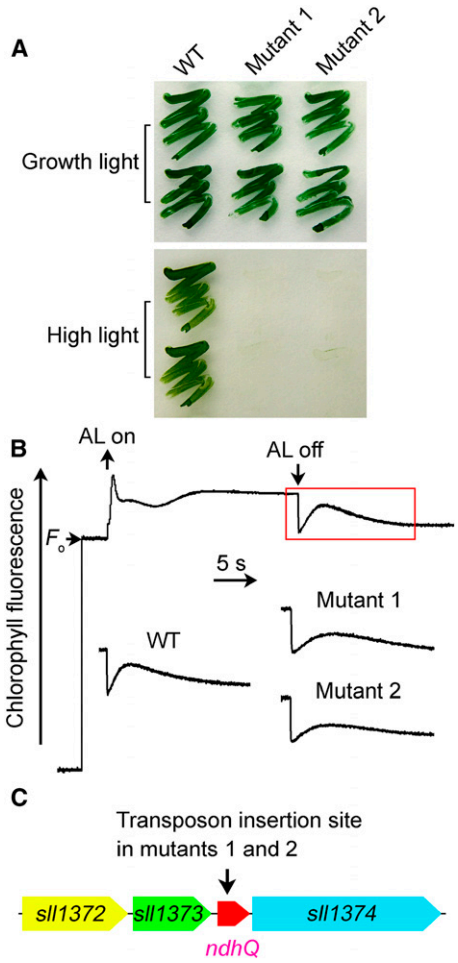

Figure 1. Use of high light condition to screen for NDH-CET-defective mutant in transposon-tagged mutant populations of *Synechocystis* 6803. A, Growth of the wild type (WT) and mutants under normal light (40 μmol photons m^{-2} s^{-1}) and high light (200 μmol photons m^{-2} s^{-1}). B, Monitoring of NDH-CET activity using Chl fluorescence analysis. The top curve shows a typical trace of Chl fluorescence in the wild-type *Synechocystis* 6803. Cells were exposed to AL (620 nm; 45 μmol photons m^{-2} s^{-1}) for 30 s. AL was turned off, and the subsequent change in the Chl fluorescence level was monitored as an indication of NDH-CET activity. C, The arrow schematically indicates the transposon insertion site in mutants 1 and 2 probed by PCR analysis using the primers listed in Supplemental Table S1.

(Mi et al., 1995; Deng et al., 2003; Ma and Mi, 2005; Battchikova et al., 2011a; Dai et al., 2013; Zhang et al., 2014; Zhao et al., 2014) and higher plants (Burrows et al., 1998; Shikanai et al., 1998; Hashimoto et al., 2003; Wang et al., 2006; Peng et al., 2009, 2011b, 2012; Sirpiö et al., 2009; Yamamoto et al., 2011; Armbruster et al., 2013). As shown in Figure 1B, the NDH-CET activity in both mutants was lower than that in the wild type as judged by the height and relative rate of postillumination increase in Chl fluorescence. The results indicate that NDH-CET is affected in mutants 1 and 2.

To identify the genes inactivated by transposon tagging, we analyzed the sites of transposon insertion

in both mutants. As shown by the PCR results (Fig. 1C), both mutants were tagged in an open reading frame identified between *sll1373* and *sll1374*. The open reading frame encodes a protein of 46 amino acids having a single-transmembrane helix (Supplemental Fig. S1), which was highly homologous to NdhQ (Supplemental Fig. S1) identified in the NDH-1L complex from *T. elongatus* using proteomics approach (Nowaczyk et al., 2011). The transposon insertion occurred at position 1842830 of the *Synechocystis* 6803 genome (Kaneko et al., 1996). This implies that inactivation of *ndhQ* impairs NDH-CET activity.

Deletion of *ndhQ* Impairs NDH-CET Activity

To confirm that inactivation of *ndhQ* impairs NDH-CET activity, we replaced the entire *ndhQ* coding region with a spectinomycin resistance marker (Sp^R; Fig. 2A). PCR analysis of the *ndhQ* locus confirmed a complete segregation of the Δ*ndhQ* mutant allele (Fig. 2B). Transcript analysis using a specific primer pair for the *ndhQ* encoding gene (see Supplemental Table S1) demonstrated the absence of gene product in the mutant (Fig. 2C). As expected, the NDH-CET activity, as measured by the postillumination increase in Chl fluorescence, was lower in Δ*ndhQ* than in the wild type. However, the activity remained relatively high compared with the M55 mutant (Fig. 2D). A similar result was obtained by measuring the oxidation of P700 by far-red light (FR) after actinic light (AL) illumination. When AL was turned off after 30-s illumination by AL (800 μmol photons m^{-2} s^{-1}) supplemented with FR, $P700^+$ was transiently reduced by electrons from the plastoquinone pool, and subsequently P700 was reoxidized by background FR. Operation of the NDH-1 complexes, which transfer electrons from the reduced cytoplasmic pool to plastoquinone, hinders the reoxidation of P700 (Shikanai et al., 1998; Battchikova et al., 2011a; Dai et al., 2013; Zhang et al., 2014; Zhao et al., 2014). The reoxidation of P700 was evidently faster in Δ*ndhQ* compared with the wild type but was much slower than in M55 (Fig. 2E). We also measured the NDH-CET by monitoring the reduction rate of $P700^+$ in darkness after illumination of cells with FR light. The rereduction of $P700^+$ was markedly slower in Δ*ndhQ* compared with that in the wild type, although it was still faster than in M55 (Fig. 2F). Furthermore, the growth of Δ*ndhQ* under high light intensities was evidently slower than the wild type, despite similar growth under growth light (Supplemental Fig. S2).

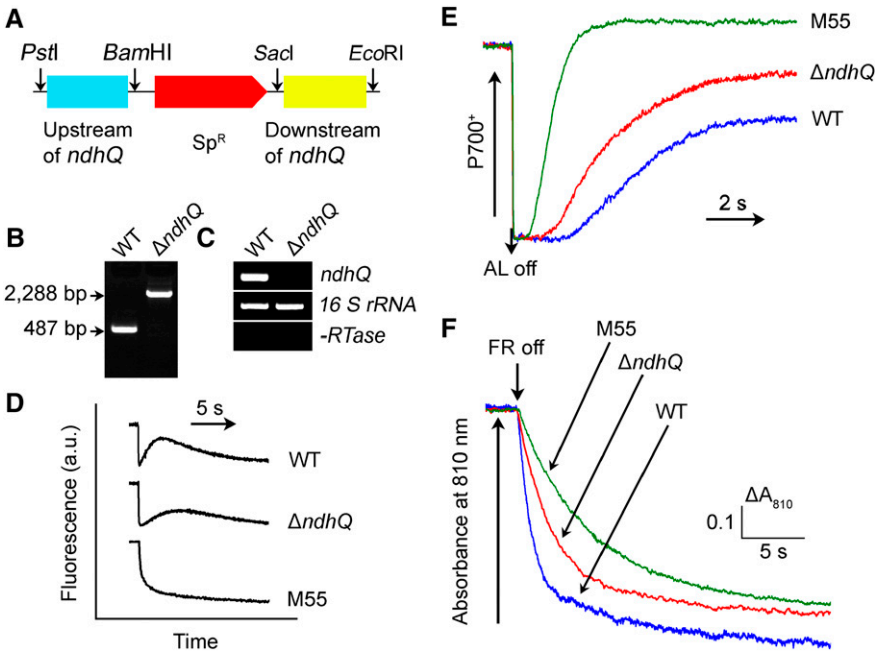

Figure 2. *ndhQ* gene deletion mutation and its effect on NDH-CET. A, Construction of the plasmid used to generate the *ndhQ*-deletion mutant (Δ*ndhQ*). B, PCR segregation analysis of the Δ*ndhQ* mutant using the *ndhQ*-G and *ndhQ*-H primers (Supplemental Table S1). C, The transcript levels of *ndhQ* in the wild-type (WT) and Δ*ndhQ* strains. The transcript level of *16 S ribosomal RNA* (*rRNA*) in each sample is shown as a control. The absence of contamination of DNA was confirmed by PCR without reverse transcriptase reaction. D, Monitoring of NDH-CET activity by Chl fluorescence. Experimental procedure as in Fig. 1. a.u., Arbitrary units. E, Redox kinetics of P700 after termination of AL illumination (800 μmol photons m^{-2} s^{-1} for 30 s) under a background of FR. The cells were illuminated by AL supplemented with FR light to store electrons in the cytoplasmic pool. After termination of AL illumination, $P700^+$ was transiently reduced by electrons from the plastoquinone pool; thereafter, P700 was reoxidized by background FR. The redox kinetics of P700 were recorded. The $P700^+$ levels were standardized by their maximum levels attained by exposure to FR light. F, Kinetics of the $P700^+$ rereduction in darkness after turning off FR in the presence of 10 μM 3-(3,4-dichlorophenyl)-1,1-dimethylurea (DCMU). The Chl *a* concentration was adjusted to 20 μg mL^{-1} before measurement, and curves are normalized to the maximal signal.

Taking these results together, we conclude that deletion of *ndhQ* impairs the NDH-CET activity.

NdhQ Is Required for Stabilization of NDH-1L Complex

To reveal how deletion of *ndhQ* impairs NDH-CET activity, we separated NDH-1L and NDH-1M complexes from thylakoid membranes of the wild type, Δ*ndhQ*, and M55 strains and deduced the amount of these complexes from the density of NdhH, NdhI, NdhK, and NdhM bands visualized by the western analyses. Deletion of *ndhQ* did not influence the abundance of total NDH-1 in the thylakoid membranes (Fig. 3A), but evidently decreased the amount of NDH-1L complex and increased that of NDH-1M complex (Fig. 3, B and C).

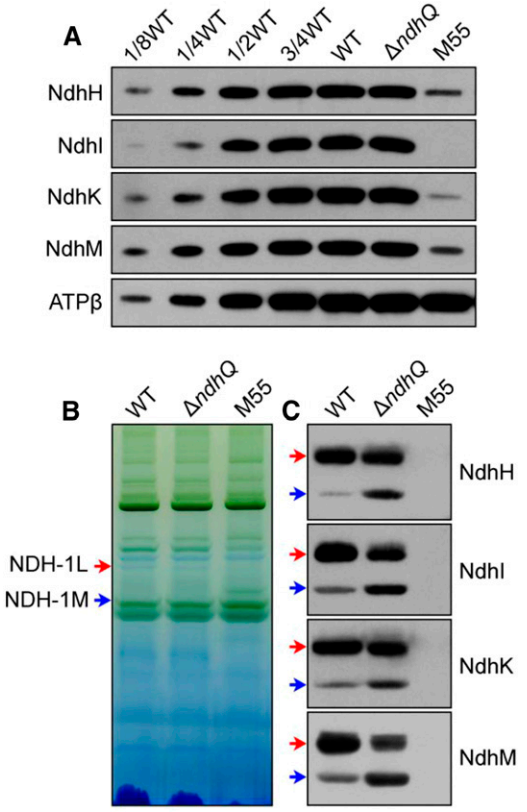

Figure 3. Western analyses of NDH-1L and NDH-1M complexes from the wild-type (WT), Δ*ndhQ*, and M55 strains. A, Immunodetection of Ndh subunits in thylakoid membranes from the wild-type (including indicated serial dilutions), Δ*ndhQ*, and M55 mutants. Immunoblotting was performed using antibodies against hydrophilic Ndh subunits (NdhH, NdhI, NdhK, and NdhM). Lanes were loaded with thylakoid membrane proteins corresponding to 1 μg of Chl *a*. In the lowest lane, ATPβ was used as a loading control. B, Thylakoid protein complexes isolated from the wild type and mutants were separated by blue native (BN)-PAGE. Thylakoid membrane extract corresponding to 9 μg of Chl *a* was loaded onto each lane. The positions of the NDH-1L and NDH-1M complexes are indicated by red and blue arrows, respectively. C, Protein complexes were electroblotted to a polyvinylidene difluoride membrane, and the membrane was cross reacted with anti-NdhH, NdhI, NdhK, and NdhM to probe the assembly of the NDH-1L and NDH-1M complexes.

The results indicated that treatment of the thylakoid membrane of the Δ*ndhQ* mutant by *n*-dodecyl-β-D-maltoside (DM) on ice disassembled the NDH-1L complex to form the NDH-1M complex, possibly by removing NdhD1, NdhF1, and NdhP, or it was already disassembled in the cells. When the treatment was continued at room temperature for 10 min, the remaining NDH-1L was almost completely disassembled into NDH-1M (Fig. 4, D–F). The thermal collapse of NDH-1L into NDH-1M was much faster in the Δ*ndhQ* mutant than in the wild type (Fig. 4). These results strongly suggested that NdhQ is present only in the NDH-1L complex, although we could not analyze the comigration of NdhQ with NDH-1 complexes because the NdhQ-yellow fluorescent protein (YFP)-His6 protein influenced the assembly and activity of the complexes (data not shown). Taken together, we may conclude that absence of NdhQ destabilizes the NDH-1L complex, thereby impairing the NDH-CET activity.

Deletion of *ndhQ* Suppresses Respiration

In addition to NDH-CET, NDH-1L is also involved in respiration, but not CO_2 uptake (Zhang et al., 2004). To consolidate this conclusion that absence of NdhQ destabilized the NDH-1L complex, we examined the effects of deletion of NdhQ on the activities of respiration and CO_2 uptake. The rate of O_2 uptake in the dark in the wild type was 23.6 ± 1.8 μmol O_2 mg^{-1} Chl *a* h^{-1}, which was reduced to 14.1 ± 1.5 μmol O_2 mg^{-1} Chl *a* h^{-1} in the Δ*ndhQ*. Consequently, the Δ*ndhQ* mutant grew slowly on the plate in the presence of Glc plus DCMU but, similar to the wild type in their absence (Fig. 5) and state 2 transition, was impaired in the mutant after the transfer of cells from light to dark (Fig. 6, A–D). Light-to-dark transition causes the reduction of plastoquinone pool by respiration, which triggers the cells into state 2 transition (Fork and Satoh, 1983; Mullineaux and Allen, 1986, 1990; Dominy and Williams, 1987). In the Δ*ndhQ* mutant, inhibition of plastoquinone pool reduction in the dark impedes the cells entering state 2 transition (Fig. 6, A–D), as observed in M55 (Fig. 6, E and F) and in the previous studies (Schreiber et al., 1995; Huang et al., 2003; Ogawa et al., 2013). Deletion of *ndhQ* did not influence the CO_2 uptake activity as deduced from the growth characteristics of Δ*ndhQ*, very similar to that of the wild type under either high CO_2 or air level of CO_2 at pH 6.5 (Supplemental Fig. S3). This finding was reinforced by the results showing that deletion of *ndhQ* did not collapse the complex of either NDH-1M (Fig. 3, B and C) or NDH-1S (Supplemental Fig. S4). Based on the aforementioned results, we conclude that deletion of *ndhQ* impaired respiration but not CO_2 uptake, which consolidates the conclusion that NdhQ stabilizes the NDH-1L complex.

NdhQ and NdhP Jointly Stabilize the NDH-1L Complex

Recently, Zhang et al. (2014) indicated that NdhP is also required to stabilize the NDH-1L complex. To test

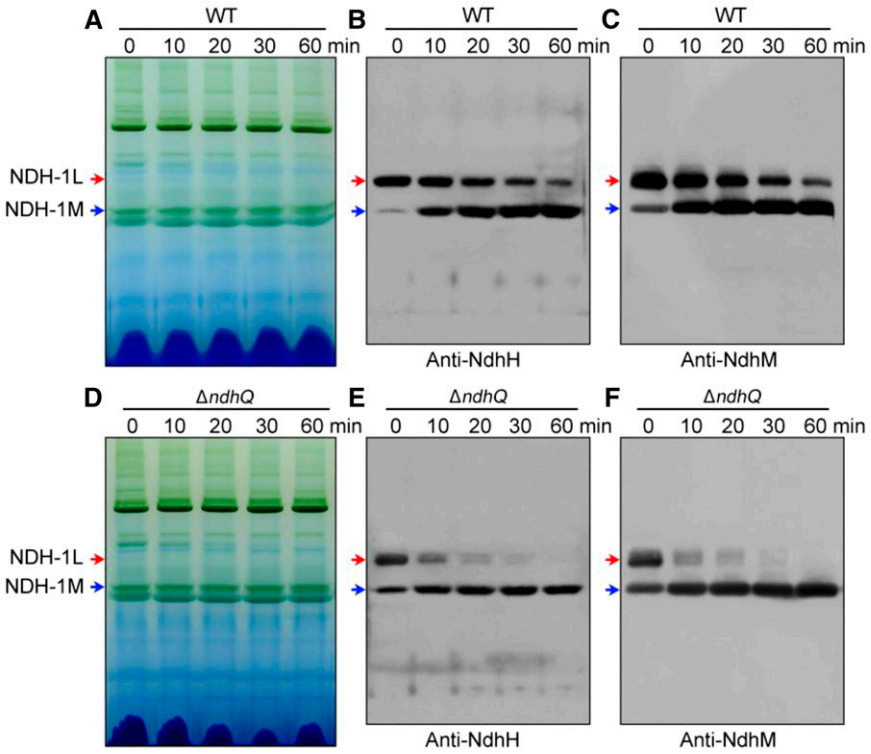

Figure 4. Effect of temperature and incubation time on the stability of NDH-1L and NDH-1M complexes from the wild-type (WT) and Δ*ndhQ* strains. A and D, Profiles of BN-PAGE of the thylakoid membranes isolated from the wild-type and Δ*ndhQ* strains. The membranes were incubated with 1.5% (w/v) DM on ice for 60 min (at 25˚C for 0 min) or at 25˚C for 10, 20, 30, and 60 min. Western analyses of NDH-1L (red arrows) and NDH-1M (blue arrows) of the wild type (B and C) and Δ*ndhQ* (E and F) isolated in A and D, using antibodies against NdhH and NdhM.

whether NdhQ and NdhP jointly stabilize the NDH-1L complex, we constructed a Δ*ndhP*/Δ*ndhQ* (Δ*P*/*Q*) double mutant strain (Supplemental Fig. S5). As deduced from the density of NdhI and NdhM bands visualized by western analyses, the NDH-1L complex was almost completely disassembled to the NDH-1M complex in the Δ*P*/*Q* mutant (Fig. 7), which was very similar to the results observed in the Δ*ndhD1*/Δ*ndhD2* (Δ*D1*/*D2*) mutant (Fig. 7) and such disassembly in the double mutant Δ*P*/*Q* was much more evident than that in its respective single mutants Δ*ndhP* (Zhang et al., 2014) and Δ*ndhQ* (Fig. 3, B and C). We therefore conclude that NdhQ and NdhP jointly stabilize the NDH-1L complex in *Synechocystis* 6803.

DISCUSSION

Over the past decade, a significant achievement has been made in identifying the composition and function of oxygenic photosynthesis-specific subunits from the NDH-1 complexes in cyanobacteria (for review, see Battchikova and Aro, 2007; Ogawa and Mi, 2007; Ma, 2009; Battchikova et al., 2011b; Ma and Ogawa, 2015) and higher plants (for review, see Suorsa et al., 2009; Ifuku et al., 2011; Peng et al., 2011a). Recently, a new oxygenic photosynthesis-specific subunit, NdhQ, was identified in the NDH-1L complex purified by Ni^{2+} affinity chromatography from *T. elongatus* (Nowaczyk et al., 2011). We found in this study that deletion of NdhQ disassembled the NDH-1L into NDH-1M and possibly NdhD1/NdhF1/NdhP, but not NDH-1MS, in the cells of *Synechocystis* 6803. The deletion impaired respiration but not CO_2 uptake, being consistent with the aforementioned result. Therefore, NdhQ appears to be present only in the NDH-1L complex.

In this study, the deletion of NdhQ disassembled about one-half of the NDH-1L to NDH-1M on ice, and the rest was completely disassembled to NDH-1M during prolonged incubation of the thylakoid membrane with DM at room temperature. By contrast, the deletion of NdhP, which is suggested to be located between NdhD1 and NdhF1 (Zhang et al., 2014), also disassembled about one-half of the NDH-1L into NDH-1M, but the rest was decomposed into small pieces without forming NDH-1M during the incubation at room temperature (Zhang et al.,

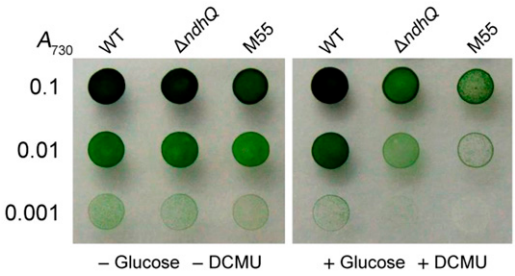

Figure 5. Photoheterotrophic growth of wild-type (WT), Δ*ndhQ*, and M55 cells on agar plates. Three microliters of cell suspensions with densities corresponding to A_{730} nm values of 0.1 (top row), 0.01 (middle row), and 0.001 (bottom row) was spotted on agar plates. Five millimolars of Glc and 10 μM DCMU were added to the plates for photoheterotrophic growth (right side) or were not added for photoautotrophic growth (left side). The plates were incubated under 2% (v/v) CO_2 in air for 6 d at 40 μmol photons m^{-2} s^{-1}.

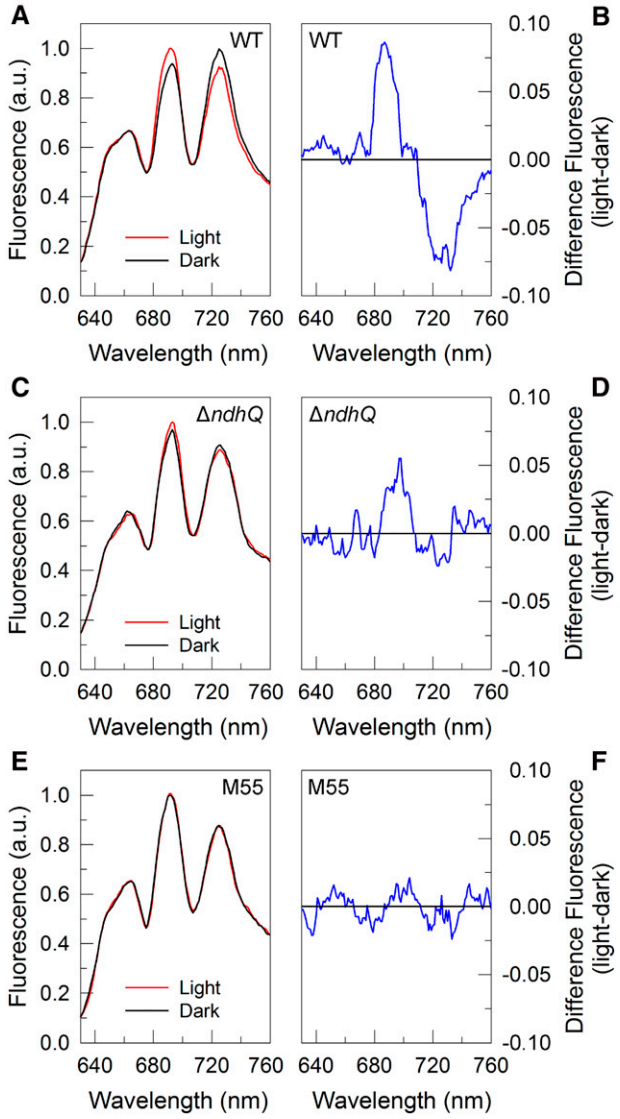

Figure 6. The 77K fluorescence emission and difference spectra in wild-type (WT), Δ*ndhQ*, and M55 cells. Fluorescence emission spectra recorded at 77K for intact wild type (A), Δ*ndhQ* (C), and M55 (E) illuminated under growth light (red line) and incubated in the dark for 10 min (black line). Difference spectra for wild-type, Δ*ndhQ*, and M55 cells are calculated as light minus dark (B, D, and F). Each spectrum is a mean of six spectra of the same sample in different tubes by exciting phycobilins at 580 nm and normalizing at 707 nm.

2014). In addition, deletion of both NdhD1 and NdhD2 completely disassembled the NDH-1L into NDH-1M, as deduced from the results of western analyses of this study and previous studies (Zhang et al., 2004, 2014). Thus, the disassembling property of NDH-1L in Δ*ndhQ* is different from that in Δ*ndhP* but similar to that in Δ*D1/D2*. This implies that NdhQ is localized between NdhB and NdhD1, as schematically represented in Figure 8.

Our results indicated that in cyanobacteria, NdhP and NdhQ jointly stabilize the NDH-1L complex, as schematically represented in Figure 8. In contrast, in

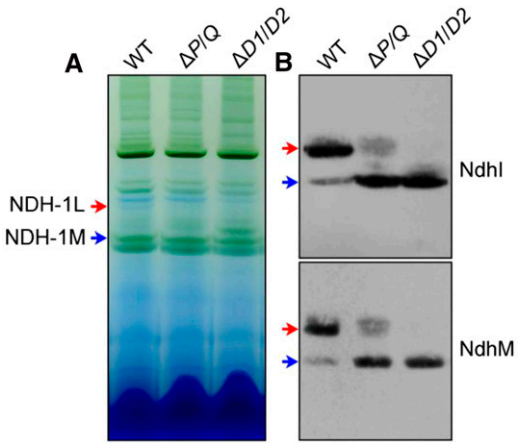

Figure 7. Western analyses of NDH-1L and NDH-1M complexes from the wild-type (WT), Δ*P/Q*, and Δ*D1/D2* strains. A, Thylakoid protein complexes isolated from the wild type and mutants were separated by BN-PAGE. Thylakoid membrane extract corresponding to 9 μg of Chl *a* was loaded onto each lane. The positions of the NDH-1L and NDH-1M complexes are indicated by red and blue arrows, respectively. B, Protein complexes were electroblotted to a polyvinylidene difluoride membrane, and the membrane was cross reacted with anti-NdhI and NdhM to probe assembly of the NDH-1L and NDH-1M complexes.

higher plants, NdhP (i.e. NDH-1-dependent flow6) is a component of subcomplex B (Ishikawa et al., 2008; Yabuta et al., 2010; Peng et al., 2011a), an exclusive NDH-1 subcomplex in higher plants (Peng et al., 2009, 2011a; Ifuku et al., 2011), and NdhQ is absent in higher plants (Nowaczyk et al., 2011). Therefore, this stabilization strategy of both NdhP and NdhQ on the NDH-1L complex is specific to cyanobacterial cells.

NDH-1M is considered to be associated with NDH-1S in the cells as a functional NDH-1MS complex, which is easily dissociated into NDH-1M and NDH-1S during solubilization of the membranes with DM, even on ice (Zhang et al., 2004, 2005). Such instability of the NDH-1MS is consistent with the absence of NdhP and NdhQ in this complex.

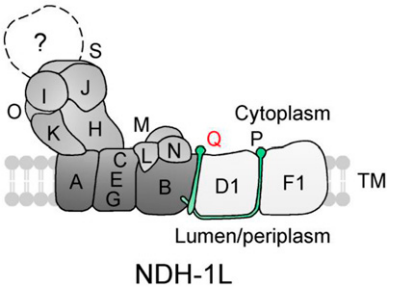

Figure 8. A model schematically represents the localization of NdhQ in the NDH-1L complex. NdhQ, which was suggested to be located between NdhB and NdhD1, together with NdhP jointly stabilize the NDH-1L complex. NdhP and NdhQ are two oxygenic photosynthesis-specific small single transmembrane subunits and are indicated by green. TM, Thylakoid membrane.

MATERIALS AND METHODS

Culture Conditions

A Glc-tolerant strain of wild-type *Synechocystis* 6803 and its mutants, Δ*ndhP* (Zhang et al., 2014), Δ*ndhQ*, Δ*P/Q*, Δ*ndhB* (M55; Ogawa, 1991), Δ*D1/D2* (Ohkawa et al., 2000), and wild type-NdhQ-YFP-His6, were cultured at 30°C in blue green (BG)-11 medium (Allen, 1968) buffered with Tris-HCl (5 mM, pH 8.0) and bubbled with 2% (v/v) CO_2 in air. Solid medium was BG-11 supplemented with 1.5% (w/v) agar. The mutant strains were grown in the presence of appropriate antibiotics under illumination by fluorescence lamps at 40 μmol photons m^{-2} s^{-1}.

Isolation and Construction of Mutants

A cosmid library of *Synechocystis* 6803 genome was constructed. The library that contained 10^5 clones with inserts of 35 to 38.5 kb was subjected to in vitro transposon mutagenesis using a EZ-Tn*5* < KAN-2 > Insertion Kit (Epicentre Biotechnologies) and then used to transform the wild-type cells of *Synechocystis* 6803. Following transformation, cells were spread on 1.5% (w/v) BG-11 agar plates supplemented with 5 μg mL^{-1} kanamycin, and kanamycin resistance mutants that grew slowly under high light but normally under growth light were isolated. Genomic DNA isolated from each mutant was digested with *Hha*I and after self ligation was used as a template for inverse PCR with primers (Supplemental Table S1) complementary to the N- and C-terminal regions of the kanamycin resistance cassette. The exact position of the cassette in the mutant genome was determined by sequencing the PCR product.

The upstream and downstream regions of *ndhQ* were amplified by PCR, creating appropriate restriction sites. A DNA fragment encoding an Sp^R cassette was also amplified by PCR, creating *Bam*HI and *Sac*I sites using PCR primers *ndhQ*-C and *ndhQ*-D (Supplemental Table S1). These three PCR products were ligated into the multiple cloning site of pUC19 (Fig. 2A) and were used to transform the wild type and Δ*ndhP* (Zhang et al., 2014) cells to generate the Δ*ndhQ* and Δ*P/Q* mutant strains. The transformants were spread on agar plates containing BG-11 medium and spectinomycin (10 μg mL^{-1}) buffered at pH 8.0, and the plates were incubated in 2% (v/v) CO_2 in air under illumination by fluorescent lamps at 40 μmol photons m^{-2} s^{-1}. The mutated *ndhQ* in the transformants was segregated to homogeneity (by successive-streak purification) as determined by PCR amplification and reverse transcription (RT)-PCR analysis (Fig. 2, B and C; Supplemental Fig. S5).

A DNA fragment containing *ndhQ* and its upstream region was amplified by PCR, creating *Sal*I and *Kpn*I sites on both ends, and was ligated to the *Sal*I and *Kpn*I sites in multiple cloning site of the pEYFP-His6-Sp^R plasmid (Birungi et al., 2010). A fragment containing the downstream region of *ndhQ* was also amplified by PCR, creating *Eco*RI and *Spe*I sites, and was ligated to the downstream of the Sp^R gene. The vector thus constructed was used to transform the wild-type cells of *Synechocystis* 6803 to generate the wild type-NdhQ-YFP-His6 mutant strain. The transformation was performed as described previously (Williams and Szalay, 1983; Long et al., 2011). The *yfp* and *his6* region in the transformants was segregated to homogeneity (by successive-streak purification) as determined by PCR amplification (data not shown).

RNA Extraction and RT-PCR Analysis

Total RNA was isolated and analyzed as described previously (McGinn et al., 2003). RT-PCR was performed using the Access RT-PCR system (Promega) to generate products corresponding to *ndhQ* and *16 S rRNA*, with 0.5 μg of DNase-treated total RNA as starting material. RT-PCR conditions were 95°C for 5 min followed by cycles of 95°C, 62°C, and 72°C for 30 s each. The reactions were stopped after 25 cycles for *16 S rRNA* and after 35 cycles for *ndhQ*. The primers used are summarized in Supplemental Table S1.

Chl Fluorescence and P700 Analysis

The transient increase in Chl fluorescence after AL had been turned off was monitored as described (Ma and Mi, 2005). The redox kinetics of a special Chl pair in the PSI reaction center (P700) was measured according to previously described methods (Battchikova et al., 2011a; Dai et al., 2013; Zhang et al., 2014; Zhao et al., 2014). The rereduction of $P700^+$ in darkness was measured with a Dual-PAM-100 (Walz) with an emitter-detector unit ED-101US/MD by monitoring absorbance changes at 830 nm and using 875 nm as a reference. Cells were kept in the dark for 2 min, and 10 μM DCMU was added to the cultures prior to the measurement. The P700 was oxidized by FR with a maximum at 720 nm from a light-emitting diode lamp for 30 s, and the subsequent rereduction of $P700^+$ in the dark was monitored.

Isolation of Crude Thylakoid Membranes

The cell cultures (5 L) were harvested at the logarithmic phase (A_{730} = 0.6–0.8) and washed twice by 50 mL of fresh BG-11 medium, and then thylakoid membranes were isolated according to Gombos et al. (1994), with some modifications as follows. Cells were suspended in 5 mL of disruption buffer (10 mM HEPES-NaOH, 5 mM sodium phosphate, pH 7.5, 10 mM $MgCl_2$, 10 mM NaCl, and 25% [v/v] glycerol), and after adding zirconia/silica beads, they were broken by vortexing 20 times at the highest speed for 30 s at 4°C with 5 min of cooling on ice between the runs. The crude extract was centrifuged at 5,000*g* for 5 min to remove the glass beads and unbroken cells. By further centrifugation at 20,000*g* for 30 min, we obtained crude thylakoid membranes from the precipitation.

Electrophoresis and Immunoblotting

BN-PAGE of *Synechocystis* 6803 membranes was performed as described previously (Kügler et al., 1997), with slight modifications (Battchikova et al., 2011a; Dai et al., 2013; Zhang et al., 2014; Zhao et al., 2014). Isolated membranes were prepared for BN-PAGE as follows. Membranes were washed with 330 mM sorbitol, 50 mM BisTris, pH 7.0, and 0.5 mM phenylmethylsulfonyl fluoride (Sigma-Aldrich), and resuspended in 20% (w/v) glycerol, 25 mM BisTris, pH 7.0, 10 mM $MgCl_2$, 0.1 units of RNase-free DNase RQ1 (Promega) at a Chl *a* concentration of 0.3 mg mL^{-1}, and 0.5 mM phenylmethylsulfonyl fluoride. The samples were incubated on ice for 10 min, and an equal volume of 3% (w/v) DM was added. Solubilization was performed for 40 min on ice. Insoluble components were removed by centrifugation at 18,000*g* for 15 min. The collected supernatant was mixed with one-tenth volume of sample buffer, 5% (w/v) Serva Blue G, 100 mM BisTris, pH 7.0, 30% (w/v) Suc, 500 mM ε-amino-*n*-caproic acid, and 10 mM EDTA. Solubilized membranes were then applied to a 0.75-mm-thick, 5% to 12.5% (w/v) acrylamide gradient gel (Hoefer Mighty Small mini-vertical unit). Samples were loaded on an equal Chl *a* basis per lane. Electrophoresis was performed at 4°C by increasing the voltage gradually from 50 V to 200 V during the 5.5-h run.

SDS-PAGE of *Synechocystis* 6803 crude thylakoid membranes was carried out on 12% (w/v) polyacrylamide gel with 6 M urea, as described earlier (Laemmli, 1970).

For immunoblotting, the proteins were electrotransferred to a polyvinylidene difluoride membrane (Immobilon-P; Millipore) and detected by protein-specific antibodies using an ECL assay kit (Amersham Pharmacia) according to the manufacturer's protocol. Antibodies against NdhH, NdhI, NdhK, NdhM, and ATPβ proteins of *Synechocystis* 6803 were previously raised in our laboratory (Ma and Mi, 2005; Zhao et al., 2014). Antibodies against NdhD3 and CupA were provided by Eva-Mari Aro (Department of Biochemistry, University of Turku) and Hualing Mi (Institute of Plant Physiology and Ecology, Chinese Academy of Sciences), respectively. Antibodies against His and GFP were purchased from Shanghai Immune Biotech Co., Ltd and Agrisera Co., respectively.

77K Fluorescence Emission Spectra

Fluorescence emission spectra at 77K of intact wild-type, Δ*ndhQ*, and M55 cells were measured using a *F*4500 spectrofluorimeter (Hitachi) at an excitation wavelength of 580 nm. Two-day-old cultures (A_{730} = 0.6–0.8) were harvested by centrifugation (5,000*g* for 5 min at 25°C), washed, and then resuspended in fresh BG-11 medium buffered with Tris-HCl (5 mM, pH 8.0) at a Chl *a* concentration of 5 μg mL^{-1}. The resuspended cultures were acclimated under the same growth conditions for 20 min. The cells were rapidly frozen in liquid nitrogen directly from either the growth light or dark adaptation for 10 min. The fluorescence spectrum was obtained by averaging six scans for each sample in different tubes. The excitation and emission slit widths were set at 5 nm, and the same capture was used in all experiments.

Supplemental Data

The following supplemental materials are available.

Supplemental Figure S1. Sequence comparison between an open reading frame product (*Synechocystis* sp. strain PCC 6803) and NdhQ (*T. elongatus*).

Supplemental Figure S2. Growth of wild-type and Δ*ndhQ* cells on the agar plates under different light intensities.

Supplemental Figure S3. Growth curve of wild-type, Δ*ndhQ*, and Δ*D3/D4* cells.

Supplemental Figure S4. Western analyses of the NDH-1S complex from the air-grown wild-type and Δ*ndhQ* cells.

Supplemental Figure S5. Identification of the Δ*P/Q* double mutant.

Supplemental Table S1. Primers used in this study.

ACKNOWLEDGMENTS

We thank Eva-Mari Aro (University of Turku) for the NdhD3 antibody and Hualing Mi (Shanghai Institutes for Biological Sciences) for the CupA antibody.

Received April 3, 2015; accepted April 14, 2015; published April 14, 2015.

LITERATURE CITED

Allen MM (1968) Simple conditions for growth of unicellular blue-green algae on plates. J Phycol **4:** 1–4

Armbruster U, Rühle T, Kreller R, Strotbek C, Zühlke J, Tadini L, Blunder T, Hertle AP, Qi Y, Rengstl B, et al (2013) The PHOTOSYNTHESIS AFFECTED MUTANT68-LIKE protein evolved from a PSII assembly factor to mediate assembly of the chloroplast NAD(P)H dehydrogenase complex in *Arabidopsis*. Plant Cell **25:** 3926–3943

Arteni AA, Zhang P, Battchikova N, Ogawa T, Aro EM, Boekema EJ (2006) Structural characterization of NDH-1 complexes of *Thermosynechococcus elongatus* by single particle electron microscopy. Biochim Biophys Acta **1757:** 1469–1475

Battchikova N, Aro EM (2007) Cyanobacterial NDH-1 complexes: multiplicity in function and subunit composition. Physiol Plant **131:** 22–32

Battchikova N, Eisenhut M, Aro EM (2011b) Cyanobacterial NDH-1 complexes: novel insights and remaining puzzles. Biochim Biophys Acta **1807:** 935–944

Battchikova N, Wei L, Du L, Bersanini L, Aro EM, Ma W (2011a) Identification of novel Ssl0352 protein (NdhS), essential for efficient operation of cyclic electron transport around photosystem I, in NADPH:plastoquinone oxidoreductase (NDH-1) complexes of *Synechocystis* sp. PCC 6803. J Biol Chem **286:** 36992–37001

Battchikova N, Zhang P, Rudd S, Ogawa T, Aro EM (2005) Identification of NdhL and Ssl1690 (NdhO) in NDH-1L and NDH-1M complexes of *Synechocystis* sp. PCC 6803. J Biol Chem **280:** 2587–2595

Bernát G, Appel J, Ogawa T, Rögner M (2011) Distinct roles of multiple NDH-1 complexes in the cyanobacterial electron transport network as revealed by kinetic analysis of $P700^+$ reduction in various *Ndh*-deficient mutants of *Synechocystis* sp. strain PCC6803. J Bacteriol **193:** 292–295

Birungi M, Folea M, Battchikova N, Xu M, Mi H, Ogawa T, Aro EM, Boekema EJ (2010) Possibilities of subunit localization with fluorescent protein tags and electron microscopy examplified by a cyanobacterial NDH-1 study. Biochim Biophys Acta **1797:** 1681–1686

Burrows PA, Sazanov LA, Svab Z, Maliga P, Nixon PJ (1998) Identification of a functional respiratory complex in chloroplasts through analysis of tobacco mutants containing disrupted plastid *ndh* genes. EMBO J **17:** 868–876

Dai H, Zhang L, Zhang J, Mi H, Ogawa T, Ma W (2013) Identification of a cyanobacterial CRR6 protein, Slr1097, required for efficient assembly of NDH-1 complexes in *Synechocystis* sp. PCC 6803. Plant J **75:** 858–866

Deng Y, Ye J, Mi H (2003) Effects of low CO_2 on NAD(P)H dehydrogenase, a mediator of cyclic electron transport around photosystem I in the cyanobacterium *synechocystis* PCC6803. Plant Cell Physiol **44:** 534–540

Dominy PJ, Williams WP (1987) The role of respiratory electron flow in the control of excitation energy distribution in blue-green algae. Biochim Biophys Acta **892:** 264–274

Endo T, Shikanai T, Takabayashi A, Asada K, Sato F (1999) The role of chloroplastic NAD(P)H dehydrogenase in photoprotection. FEBS Lett **457:** 5–8

Fork DC, Satoh K (1983) State I–state II transitions in the thermophilic blue-green alga (cyanobacterium) *Synechococcus lividus*. Photochem Photobiol **37:** 421–427

Friedrich T, Scheide D (2000) The respiratory complex I of bacteria, archaea and eukarya and its module common with membrane-bound multisubunit hydrogenases. FEBS Lett **479:** 1–5

Friedrich T, Steinmüller K, Weiss H (1995) The proton-pumping respiratory complex I of bacteria and mitochondria and its homologue in chloroplasts. FEBS Lett **367:** 107–111

Gombos Z, Wada H, Murata N (1994) The recovery of photosynthesis from low-temperature photoinhibition is accelerated by the unsaturation of membrane lipids: a mechanism of chilling tolerance. Proc Natl Acad Sci USA **91:** 8787–8791

Hashimoto M, Endo T, Peltier G, Tasaka M, Shikanai T (2003) A nucleus-encoded factor, CRR2, is essential for the expression of chloroplast *ndhB* in Arabidopsis. Plant J **36:** 541–549

Herranen M, Battchikova N, Zhang P, Graf A, Sirpiö S, Paakkarinen V, Aro EM (2004) Towards functional proteomics of membrane protein complexes in *Synechocystis* sp. PCC 6803. Plant Physiol **134:** 470–481

Huang C, Yuan X, Zhao J, Bryant DA (2003) Kinetic analyses of state transitions of the cyanobacterium *Synechococcus* sp. PCC 7002 and its mutant strains impaired in electron transport. Biochim Biophys Acta **1607:** 121–130

Ifuku K, Endo T, Shikanai T, Aro EM (2011) Structure of the chloroplast NADH dehydrogenase-like complex: nomenclature for nuclear-encoded subunits. Plant Cell Physiol **52:** 1560–1568

Ishikawa N, Takabayashi A, Ishida S, Hano Y, Endo T, Sato F (2008) NDF6: a thylakoid protein specific to terrestrial plants is essential for activity of chloroplastic NAD(P)H dehydrogenase in Arabidopsis. Plant Cell Physiol **49:** 1066–1073

Kaneko T, Sato S, Kotani H, Tanaka A, Asamizu E, Nakamura Y, Miyajima N, Hirosawa M, Sugiura M, Sasamoto S, et al (1996) Sequence analysis of the genome of the unicellular cyanobacterium *Synechocystis* sp. strain PCC6803. II. Sequence determination of the entire genome and assignment of potential protein-coding regions. DNA Res **3:** 109–136

Kügler M, Jänsch L, Kruft V, Schmitz UK, Braun HP (1997) Analysis of the chloroplast protein complexes by blue-native polyacrylamide gel electrophoresis (BN-PAGE). Photosynth Res **53:** 35–44

Laemmli UK (1970) Cleavage of structural proteins during the assembly of the head of bacteriophage T4. Nature **227:** 680–685

Long Z, Zhao J, Zhang J, Wei L, Wang Q, Ma W (2011) Effects of different light treatments on the natural transformation of *Synechocystis* sp. strain PCC 6803. Afr J Microbiol Res **5:** 3603–3610

Ma W (2009) Identification, regulation and physiological functions of multiple NADPH dehydrogenase complexes in cyanobacteria. Front Biol China **4:** 137–142

Ma W, Mi H (2005) Expression and activity of type 1 NAD(P)H dehydrogenase at different growth phases of the cyanobacterium, *Synechocystis* PCC 6803. Physiol Plant **125:** 135–140

Ma W, Ogawa T (2015) Oxygenic photosynthesis-specific subunits of cyanobacterial NADPH dehydrogenases. IUBMB Life **67:** 3–8

McGinn PJ, Price GD, Maleszka R, Badger MR (2003) Inorganic carbon limitation and light control the expression of transcripts related to the CO_2-concentrating mechanism in the cyanobacterium *Synechocystis* sp. strain PCC6803. Plant Physiol **132:** 218–229

Mi H, Endo T, Ogawa T, Asada K (1995) Thylakoid membrane-bound, NADPH-specific pyridine nucleotide dehydrogenase complex mediates cyclic electron transport in the cyanobacterium *Synechocystis* sp. PCC 6803. Plant Cell Physiol **36:** 661–668

Mi H, Endo T, Schreiber U, Ogawa T, Asada K (1992) Electron donation from cyclic and respiratory flows to the photosynthetic intersystem chain is mediated by pyridine nucleotide dehydrogenase in the cyanobacterium *Synechocystis* PCC 6803. Plant Cell Physiol **33:** 1233–1237

Mullineaux CW, Allen JF (1986) The state 2 transition in the cyanobacterium *Synechococcus* 6301 can be driven by respiratory electron flow into the plastoquinone pool. FEBS Lett **205:** 155–160

Mullineaux CW, Allen JF (1990) State 1-State 2 transitions in the cyanobacterium *Synechococcus* 6301 are controlled by the redox state of electron carriers between Photosystems I and II. Photosynth Res **23:** 297–311

Nowaczyk MM, Wulfhorst H, Ryan CM, Souda P, Zhang H, Cramer WA, Whitelegge JP (2011) NdhP and NdhQ: two novel small subunits of the cyanobacterial NDH-1 complex. Biochemistry **50:** 1121–1124

Ogawa T (1991) A gene homologous to the subunit-2 gene of NADH dehydrogenase is essential to inorganic carbon transport of *Synechocystis* PCC6803. Proc Natl Acad Sci USA **88:** 4275–4279

Ogawa T, Harada T, Ozaki H, Sonoike K (2013) Disruption of the *ndhF1* gene affects Chl fluorescence through state transition in the Cyanobacterium *Synechocystis* sp. PCC 6803, resulting in apparent high efficiency of photosynthesis. Plant Cell Physiol **54:** 1164–1171

Ogawa T, Mi H (2007) Cyanobacterial NADPH dehydrogenase complexes. Photosynth Res **93:** 69–77

Ohkawa H, Pakrasi HB, Ogawa T (2000) Two types of functionally distinct NAD(P)H dehydrogenases in *Synechocystis* sp. strain PCC6803. J Biol Chem **275:** 31630–31634

Ohkawa H, Sonoda M, Hagino N, Shibata M, Pakrasi HB, Ogawa T (2002) Functionally distinct NAD(P)H dehydrogenases and their membrane localization in *Synechocystis* sp. PCC6803. Funct Plant Biol **29:** 195–200

Ohkawa H, Sonoda M, Shibata M, Ogawa T (2001) Localization of NAD (P)H dehydrogenase in the cyanobacterium *Synechocystis* sp. strain PCC 6803. J Bacteriol **183:** 4938–4939

Peng L, Fukao Y, Fujiwara M, Shikanai T (2012) Multistep assembly of chloroplast NADH dehydrogenase-like subcomplex A requires several nucleus-encoded proteins, including CRR41 and CRR42, in *Arabidopsis*. Plant Cell **24:** 202–214

Peng L, Fukao Y, Fujiwara M, Takami T, Shikanai T (2009) Efficient operation of NAD(P)H dehydrogenase requires supercomplex formation with photosystem I via minor LHCI in *Arabidopsis*. Plant Cell **21:** 3623–3640

Peng L, Fukao Y, Myouga F, Motohashi R, Shinozaki K, Shikanai T (2011b) A chaperonin subunit with unique structures is essential for folding of a specific substrate. PLoS Biol **9:** e1001040

Peng L, Yamamoto H, Shikanai T (2011a) Structure and biogenesis of the chloroplast NAD(P)H dehydrogenase complex. Biochim Biophys Acta **1807:** 945–953

Prommeenate P, Lennon AM, Markert C, Hippler M, Nixon PJ (2004) Subunit composition of NDH-1 complexes of *Synechocystis* sp. PCC 6803: identification of two new *ndh* gene products with nuclear-encoded homologues in the chloroplast Ndh complex. J Biol Chem **279:** 28165–28173

Schreiber U, Endo T, Mi H, Asada K (1995) Quenching analysis of chlorophyll fluorescence by the saturation pulse method: particular aspects relating to the study of eukaryotic algae and cyanobacteria. Plant Cell Physiol **36:** 873–882

Shikanai T (2007) Cyclic electron transport around photosystem I: genetic approaches. Annu Rev Plant Biol **58:** 199–217

Shikanai T, Endo T, Hashimoto T, Yamada Y, Asada K, Yokota A (1998) Directed disruption of the tobacco *ndhB* gene impairs cyclic electron flow around photosystem I. Proc Natl Acad Sci USA **95:** 9705–9709

Sirpiö S, Allahverdiyeva Y, Holmström M, Khrouchtchova A, Haldrup A, Battchikova N, Aro EM (2009) Novel nuclear-encoded subunits of the chloroplast NAD(P)H dehydrogenase complex. J Biol Chem **284:** 905–912

Suorsa M, Sirpiö S, Aro EM (2009) Towards characterization of the chloroplast NAD(P)H dehydrogenase complex. Mol Plant **2:** 1127–1140

Wang P, Duan W, Takabayashi A, Endo T, Shikanai T, Ye JY, Mi H (2006) Chloroplastic NAD(P)H dehydrogenase in tobacco leaves functions in alleviation of oxidative damage caused by temperature stress. Plant Physiol **141:** 465–474

Williams JGK, Szalay AA (1983) Stable integration of foreign DNA into the chromosome of the cyanobacterium *Synechococcus* R2. Gene **24:** 37–51

Wulfhorst H, Franken LE, Wessinghage T, Boekema EJ, Nowaczyk MM (2014) The 5 kDa protein NdhP is essential for stable NDH-1L assembly in *Thermosynechococcus elongatus*. PLoS ONE **9:** e103584

Xu M, Ogawa T, Pakrasi HB, Mi H (2008) Identification and localization of the CupB protein involved in constitutive CO_2 uptake in the cyanobacterium, *Synechocystis* sp. strain PCC 6803. Plant Cell Physiol **49:** 994–997

Yabuta S, Ifuku K, Takabayashi A, Ishihara S, Ido K, Ishikawa N, Endo T, Sato F (2010) Three PsbQ-like proteins are required for the function of the chloroplast NAD(P)H dehydrogenase complex in Arabidopsis. Plant Cell Physiol **51:** 866–876

Yamamoto H, Peng L, Fukao Y, Shikanai T (2011) An Src Homology 3 Domain-Like fold protein forms a ferredoxin binding site for the chloroplast NADH dehydrogenase-like complex in *Arabidopsis*. Plant Cell **23:** 1480–1493

Zhang J, Gao F, Zhao J, Ogawa T, Wang Q, Ma W (2014) NdhP is an exclusive subunit of large complex of NADPH dehydrogenase essential to stabilize the complex in *Synechocystis* sp. strain PCC 6803. J Biol Chem **289:** 18770–18781

Zhang P, Battchikova N, Jansen T, Appel J, Ogawa T, Aro EM (2004) Expression and functional roles of the two distinct NDH-1 complexes and the carbon acquisition complex NdhD3/NdhF3/CupA/Sll1735 in *Synechocystis* sp PCC 6803. Plant Cell **16:** 3326–3340

Zhang P, Battchikova N, Paakkarinen V, Katoh H, Iwai M, Ikeuchi M, Pakrasi HB, Ogawa T, Aro EM (2005) Isolation, subunit composition and interaction of the NDH-1 complexes from *Thermosynechococcus elongatus* BP-1. Biochem J **390:** 513–520

Zhao J, Gao F, Zhang J, Ogawa T, Ma W (2014) NdhO, a subunit of NADPH dehydrogenase, destabilizes medium size complex of the enzyme in *Synechocystis* sp. strain PCC 6803. J Biol Chem **289:** 26669–26676